

DESIGN OF A MODULAR COST-EFFECTIVE ROBOT ARM FOR INCREASED DEXTERITY IN LAPAROSCOPIC SURGERY

John Lowery
Carl A. Nelson¹

Department of Mechanical & Materials Engineering
University of Lincoln, Nebraska
Lincoln, NE, USA

ABSTRACT

This paper outlines the design of a reconfigurable, partially disposable, tendon-driven robotic arm for providing assistance in laparoscopic surgery. The rationale for its development and design objectives are provided, followed by a description of its mechanical design. Kinematic simulations to assess workspace are presented, and a first-stage assessment of the functionality of a prototype using a custom test bench is also included.

INTRODUCTION

Minimally invasive laparoscopic surgery has served as an excellent alternative to traditional open surgery, as this technique has greatly reduced the required size of incisions (10mm incisions as opposed to 6-12cm). Developed in the 1980s, it has since revolutionized modern surgical practice, markedly reducing recovery times and risk of infection [1]. However, while yielding excellent results, this technique also presents a new challenge, as the size of the incisions significantly constrains surgeons' dexterity within the workspace. In order to reach through small incisions to the target area, surgeons are forced to use long, rigid instruments.

Robotic systems have been developed to address this issue and return some dexterity to the surgeon. However, these systems are typically very expensive and cannot easily be afforded by smaller clinics, restricting patient access. The most well-known example of this is the Da Vinci Surgical System (DVSS). As of 2014, only one quarter of U.S. hospitals owned a DVSS [2]. Furthermore, this robot requires straight-line access and therefore cannot necessarily cover a broad workspace, depending on the line of approach. As a result, the DVSS, like other surgical robots, is only optimized for a limited range of procedure types, for which it has distinguished itself.

We have previously reported the development of a modular, tendon-driven robot with an articulated arm designed to address these issues [3]. This first design iteration served as a useful proof-of-concept model of tendon actuation utilizing elastic antagonists. Further, the objective of minimized cost was achieved, even to the point at which disposal of the inserted portion of the robot was not prohibitively costly. However, while this robot utilized a modular port which could accommodate a range of different tool arms, the kinematics of the arms themselves could not be reconfigured. Therefore, the robot's ability to adapt to a variety of procedural demands was limited. Also, although the cable routing produced full functionality, it would ideally have allowed a constant moment arm throughout the rotation of certain joints, kept the tendons within the body of the arm and minimized friction.

Based on this first proof-of-concept model, we develop a second iteration of this low-cost alternative surgical system with a particular emphasis on adaptive configurability and optimized cable routing. The general objective is to create a disposable surgical robot which could be custom-assembled from a kit of modular subunits to comply with the procedure-specific constraints of a range of laparoscopic operations.

METHODS

The objectives detailed above are realized in the robot design through implementation of tendon-driven actuation. This allows the electric actuators to remain outside of the workspace, reducing regulatory oversight and eliminating the need for expensive, high-performance motors embedded in the system. Aside from lowering costs overall, this particularly reduces the cost associated with the inserted portion of the robot, easily lending the robot arm to single use.

The robot arm is driven by four tendons and allows 3 degrees of freedom (roll, pitch and yaw) provided by two hinge

¹ Contact author: cnelson5@unl.edu

joints and a roll joint, each of which are independently actuated by a drive tendon. The fourth tendon actuates the end-effector (a grasper). Figure 2 shows the overall structure of the arm and highlights the degrees of freedom.

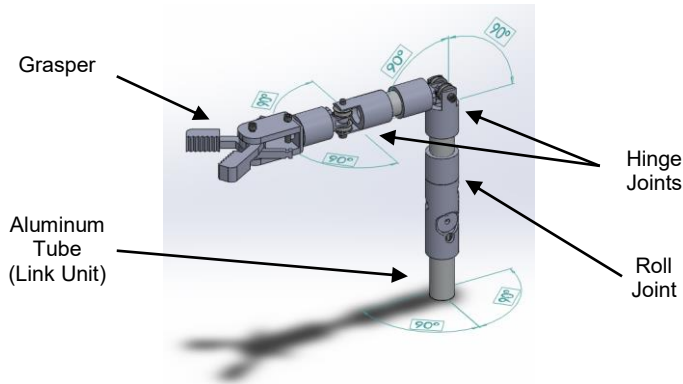


FIGURE 1: ROBOT ARM STRUCTURE & DEGREES OF FREEDOM

Figure 2 details the basic joint actuation mechanism. A fixed pulley is centered on the rotation axis of each hinge joint. An agonist tendon (drive tendon) wraps around this pulley and is fixed to it, while an antagonist tendon wraps about the same pulley in the opposite direction. The drive tendons attach to external actuators. However, in order to simplify cable routing through the length of the arm, rather than eight externally actuated tendons (4 agonist/antagonist pairs), the antagonist tendons are instead driven by elastic antagonists embedded in the arm. Freely rotating pulleys on either side of the hinge joint's drive pulley route passive cables (tendons which actuate more distal joints) through the joint. With this pulley system, the degrees of freedom are largely decoupled and the drive tendons are contained within the body of the robot.

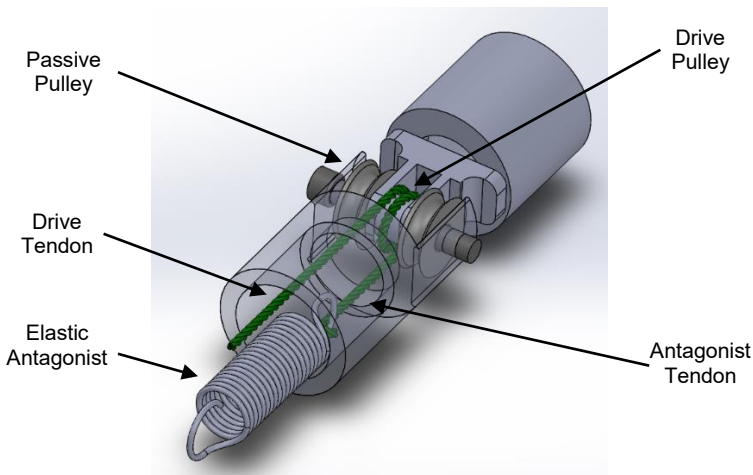


FIGURE 2: HINGE JOINT TENDON ROUTING DIAGRAM

The roll joint functions on these same principles. As shown in Figure 3, the agonist / antagonist pair wrap a double-groove pulley which is fixed to a spindle rotating on two bearings and contained within an outer sheath. Though not explicitly shown, the tendons route straight through the wall of the sheath perpendicular to the central axis of the joint and then travel down the outside to enter once again through angled holes. One attaches to the elastic antagonist while the other continues in the proximal direction to attach to the appropriate external actuator. The passive cables are allowed to simply route straight through the center of the rotating spindle.

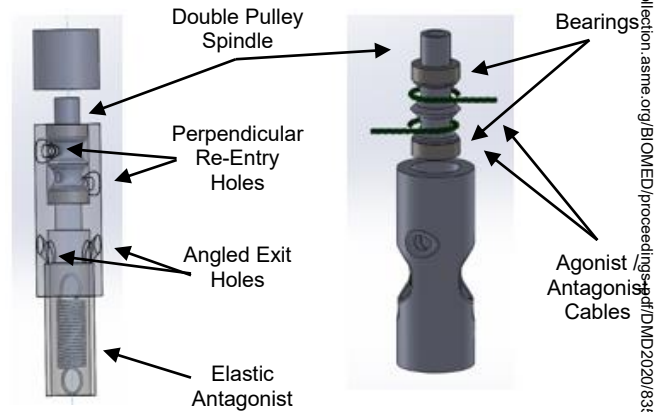


FIGURE 3: ROLL JOINT: EXPLODED PARTS DIAGRAM (LEFT) & TENDON ROUTING DIAGRAM (RIGHT)

Regarding the grasper, a tendon pair routes around a center pin to achieve tension perpendicular to the central axis of the arm, both of which are driven by a single drive tendon. The elastic antagonist in this case is embedded between the jaws of the grasper as shown in Figure 4.

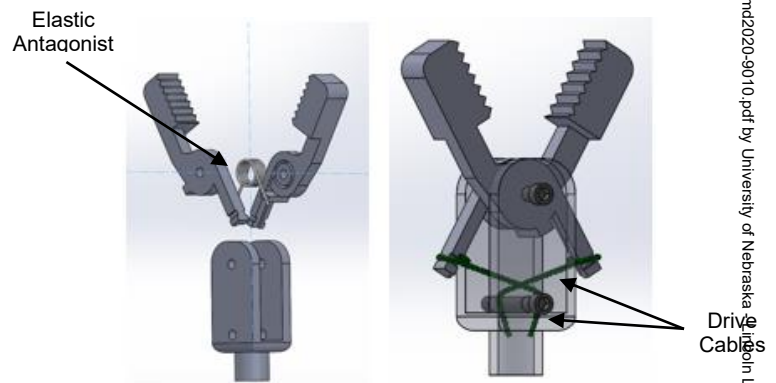


FIGURE 4: GRASPER: EXPLODED PARTS DIAGRAM (LEFT) & TENDON ROUTING DIAGRAM (RIGHT)

Though the target diameter for this robot is 10mm, this proof-of-concept model is scaled up in size and has a diameter of 12.7 mm. This is partly due to the fabrication method (3D printing using PLA) and associated feature size constraints.

While this method did not conform ideally with the targeted size constraint, it was very cost-effective, allowing the robot arm to be constructed for less than 40 US dollars. This was done by limiting the number of required custom parts and employing an inexpensive fabrication method. Other materials utilized included off-the-shelf bearings, pins and tubing as well as braided fishing line.

A test bench consisting of a base plate, interface port and four ratchets was constructed and used to independently tension the four tendons in preliminary testing. A photo of the device mounted on this test bench is provided in Figure 5.

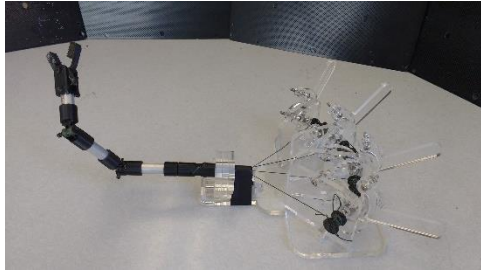


FIGURE 5: FULLY ASSEMBLED ARM MOUNTED ON TEST LEVER BENCH

Modularity is also incorporated into the design. Aside from serving as a housing for the antagonist springs and an enclosure through which the drive cables route, the aluminum tube also functions as a common link mechanism between each of the joints. Each module, therefore, consists of a joint and the linking tube containing that joint's elastic antagonist. With this design, the position of the joints can be altered relative to the end effector to create different kinematic configurations.

To complement the hardware development, simulations were created to determine how this modularity influences robot workspace. Specifically, four-link, four-joint serial robot configurations were simulated with randomly selected straight or L-shaped links, having randomized link lengths in the range of 1-8 cm, allowing four different joint axis orientations in the plane normal to the end of each link. The range of motion allowed by each joint was $\pm 90^\circ$. Standard robot kinematic transformations were programmed in MATLAB, and 200 points were randomly sampled for each configuration, with the *alphaShape()* function used to convert the resulting point cloud to a meshed volume for visualization. Figure 6 shows four randomly generated examples of shape and volume variations in the resulting workspaces. It can be noted that although all workspaces have a round or cup-like shape, as is typical for a revolute-jointed serial robot, the third workspace shown is relatively flatter. The workspace volumes also vary; for example, the third and fourth workspace volumes differ by a factor of about one-third.

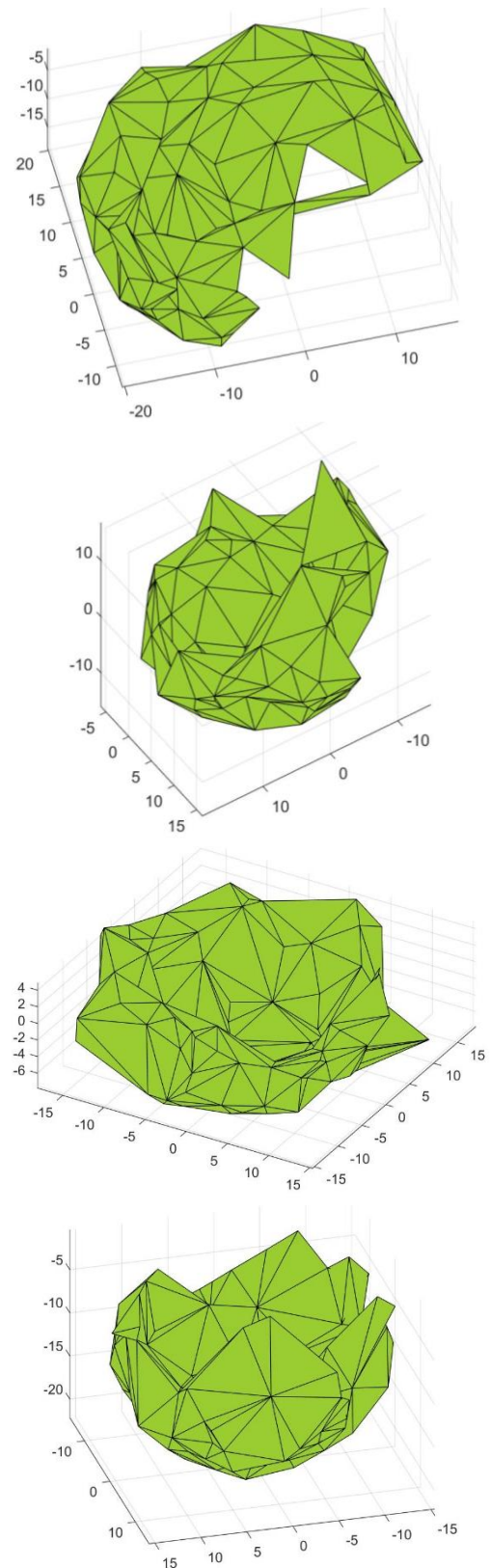


FIGURE 6: EXAMPLES OF WORKSPACE SIMULATION RESULTS (AXIS UNITS = CM)

RESULTS AND DISCUSSION

Each individual joint as well as the grasper instrument achieved the desired range of motion (shown in Figure 1) and could be effectively actuated using the drive cable / antagonist spring system. When integrated into the fully assembled arm, however, the springs utilized in this model proved to be insufficiently stiff. Therefore, though joints could be moved in a full 180-degree arc from their rest position, the springs were not strong enough to overcome the weight of the arm and return the joint back along this arc to the rest position. However, full functionality in this respect could be achieved simply by using stiffer springs.

A second barrier to achieving the desired functionality in this design was the presence of a small amount of joint coupling. As the hinge joints ranged about their axes, the drive cables routing around the passive pulleys on either side of the joint were forced to either unwrap slightly or wrap further about these passive pulleys (depending on the direction of the joint motion). The resulting changing tension in these cables gave rise to a certain degree of joint coupling. Mathematical modeling of this kinematic relationship is provided in one of our previous papers [4]. While this is an inevitable effect of the design, it can be compensated for through implementation of kinematic adjustments in the motor control, as later discussed.

This device incorporated the modularity principle discussed above. Since each module was self-contained and connected via a common linking system, the joints could be successfully attached in any order. However, configurability was limited by tendon routing. Since the hinge joints were only designed to allow two passive cables to pass through, they could not be placed at position 1 on the arm (the position nearest the test bench), as this would require routing 3 cables through the hinge joint.

A summary of the key design improvements is provided in Figure 7.

Design Parameter	1 st Iteration	2 nd Iteration	Improvement
Cable Routing Path	Along Exterior of Body / Joints	Contained within Body	Reduced Risk of Interference with Environment
Routing Mechanism	Guide Eyelets	Pulleys	Reduced Friction / Predictable Passive Cable Tensioning
Cable Attachment about Joints	Fixed Exterior Point Attachment	Wrap Center Drive Pulleys	Constant Rotational Moment Arm
Subunit Architecture	Not Modular, Individualized Connections	Modular, Common Link Mechanism	Reconfigurable
Elastic Antagonist	Rubber Band	Metal Spring	Increased Strength / Durability

FIGURE 7: SUMMARY OF PRIMARY DESIGN IMPROVEMENTS IN 2ND DESIGN ITERATION (THIS ARTICLE) AS COMPARED TO 1ST ITERATION [3].

CONCLUSIONS

The robot design presented satisfies cost constraints and is conducive to reconfiguration and single use. While full modularity is not yet implemented, only one feature will require modification in order for this to be achieved. In addition, since the device does not rely on actuators directly integrated into the tool arm, it is not prohibitively costly to dispose of the arm after one use.

The cable routing pulley system employed in this design will also allow for simple implementation of motor control. In this pulley system, the rotational moment arm by which the joint is manipulated remains independent of joint rotation, therefore maintaining a constant value: the radius of the drive pulley. Similarly, due to the constant radius of the routing pulleys, the inevitable tensioning / slackening (wrapping / unwrapping) of the passive cables as a result of joint rotation occurs in a predictable manner [4]. These factors will allow for the development of a precise control algorithm.

Future work would involve development of motor control of the device's four degrees of freedom. However, another primary focus would also be increasing the maximum number of passive cables allowed to route through the hinge joint. Configuration modularity may also be explored further to determine preferred configurations for workspace requirements pertinent to particular surgical procedures.

ACKNOWLEDGEMENTS

Funding provided by National Science Foundation Award No. 1659777.

REFERENCES

- [1] Kelley, W. E. Jr., 2008, "The evolution of laparoscopy and the revolution in surgery in the decade of the 1990s." *JSLIS: Journal of the Society of Laparoendoscopic Surgeons* 12(4): 351-357.
- [2] ECRI, 2015, "Robotic Surgery Infographic," https://www.ecri.org/Resources/ASG/Robotic_Surgery_Infographic_MS15369_web.pdf
- [3] Nelson, N., Nelson, C. A., 2018, "Design of a Modular, Partially Disposable Robot for Minimally Invasive Surgery," ASME Design of Medical Devices Conference, Minneapolis, MN, April 10-12, 2018, paper number DMD2018-6821.
- [4] Nelson, C. A., 2018, "A Modular Cable-Driven Robot with a Safe Joint Design," 4th IFToMM Symposium on Mechanism Design for Robotics (MEDER 2018), Udine, Italy, Sept. 11-13, 2018.